Decay properties of tau leptons measured at the Z0 resonance

Adeva, B.; Adriani, O.; Aguilar-Benitez, M.; Ahlen, S.P.; Akbari, H.; Alcaraz, J.; Aloisio, A.; Alverson, G.; Linde, F.L.

Published in:
Physics Letters B

DOI:
10.1016/0370-2693(91)90081-Z

Physics Letters B 265 (1991) 451–461
North-Holland

PHYSICS LETTERS B

Decay properties of tau leptons measured at the Z^0 resonance

L3 Collaboration

B. Adeva [a], O. Adriani [b], M. Aguilar-Benitez [c], H. Akbari [d], J. Alcaraz [c], A. Aloisio [e], G. Alverson [f], M.G. Alviggi [e], G. Ambrosi [g], Q. An [h], H. Anderhub [i], A.L. Anderson [j], V.P. Andreev [k], T. Angelov [j], L. Antonov [ℓ], D. Antreasyan [m], P. Arce [c], A. Arefiev [n], T. Azemoon [o], T. Aziz [p], P.V.K.S. Baba [h], P. Bagnaia [q], J.A. Bakken [r], L. Baksay [s], R.C. Ball [o], S. Banerjee [p], J. Bao [d], R. Barillère [a], L. Barone [q], R. Battiston [g], A. Bay [t], U. Becker [j], F. Behner [i], J. Behrens [i], S. Beingessner [u], Gy.L. Bencze [a,v], J. Berdugo [c], P. Berges [j], B. Bertucci [g], B.L. Betev [ℓ], A. Biland [i], G.M. Bilei [g], R. Bizzarri [q], J.J. Blaising [u], P. Blömeke [w], B. Blumenfeld [d], G.J. Bobbink [x], M. Bocciolini [b], R. Bock [w], A. Böhm [a,w], B. Borgia [q], D. Bourilkov [ℓ], M. Bourquin [t], D. Boutigny [u], B. Bouwens [x], J.G. Branson [y], I.C. Brock [z], F. Bruyant [a], C. Buisson [aa], A. Bujak [ab], J.D. Burger [j], J.P. Burq [aa], J. Busenitz [s], X.D. Cai [h], M. Capell [ac], F. Carbonara [e], M. Caria [g], F. Carminati [b], A.M. Cartacci [b], M. Cerrada [c], F. Cesaroni [q], Y.H. Chang [j], U.K. Chaturvedi [h], M. Chemarin [aa], A. Chen [ad], C. Chen [ae], G.M. Chen [ae], H.F. Chen [af], H.S. Chen [ae], M. Chen [j], M.L. Chen [o], W.Y. Chen [h], G. Chiefari [e], C.Y. Chien [d], M. Chmeissani [o], C. Civinini [b], I. Clare [j], R. Clare [j], H.O. Cohn [ag], G. Coignet [u], N. Colino [a], V. Commichau [w], G. Conforto [b], A. Contin [a,m], F. Crijns [ah], X.Y. Cui [h], T.S. Dai [j], R. D'Alessandro [b], R. de Asmundis [e], A. Degré [u,a], K. Deiters [j], E. Dénes [a,v], P. Denes [r], F. DeNotaristefani [q], M. Dhina [i], D. DiBitonto [s], M. Diemoz [q], H.R. Dimitrov [ℓ], C. Dionisi [q], M.T. Dova [h], E. Drago [e], T. Driever [ah], D. Duchesneau [t], P. Duinker [x], I. Duran [c], H. El Mamouni [aa], A. Engler [z], F.J. Eppling [j], F.C. Erné [x], P. Extermann [t], R. Fabbretti [ai], M. Fabre [i], S. Falciano [q], Q. Fan [h], S.J. Fan [aj], O. Fackler [ac], J. Fay [aa], T. Ferguson [z], G. Fernandez [c], F. Ferroni [a,q], H. Fesefeldt [w], E. Fiandrini [g], J. Field [t], F. Filthaut [ah], G. Finocchiaro [q], P.H. Fisher [d], G. Forconi [t], T. Foreman [x], K. Freudenreich [i], W. Friebel [ak], M. Fukushima [j], M. Gailloud [a,ℓ], Yu. Galaktionov [n], E. Gallo [b], S.N. Ganguli [p], P. Garcia-Abia [c], S.S. Gau [ad], D. Gele [aa], S. Gentile [q], M. Glaubman [f], S. Goldfarb [o], Z.F. Gong [af], E. Gonzalez [c], A. Gordeev [n], P. Göttlicher [w], D. Goujon [t], G. Gratta [am], C. Grinnell [j], M. Gruenewald [am], M. Guanziroli [h], J.K. Guo [aj], A. Gurtu [p], H.R. Gustafson [o], L.J. Gutay [ab], H. Haan [w], A. Hasan [h], D. Hauschildt [x], C.F. He [aj], T. Hebbeker [w], M. Hebert [y], G. Herten [j], U. Herten [w], A. Hervé [a], K. Hilgers [w], H. Hofer [i], H. Hoorani [h], L.S. Hsu [ad], G. Hu [h], G.Q. Hu [aj], B. Ille [aa], M.M. Ilyas [h], V. Innocente [a,e], H. Janssen [a], S. Jezequel [u], B.N. Jin [ae], L.W. Jones [o], A. Kasser [a,ℓ], R.A. Khan [h], Yu. Kamyshkov [ag,n], Y. Karyotakis [a,u], M. Kaur [h], S. Khokhar [h], V. Khoze [k], M.N. Kienzle-Focacci [t], W. Kinnison [an], D. Kirkby [am], W. Kittel [ah], A. Klimentov [n], A.C. König [ah], O. Kornadt [w], V. Koutsenko [j,n], R.W. Kraemer [z], T. Kramer [j], V.R. Krastev [ℓ], W. Krenz [w], J. Krizmanic [d], K.S. Kumar [ao], V. Kumar [h], A. Kunin [n,ao], V. Lalieu [t], G. Landi [b], K. Lanius [a], D. Lanske [w], S. Lanzano [e], P. Lebrun [aa], P. Lecomte [i], P. Lecoq [a], P. Le Coultre [i], D. Lee [an], I. Leedom [f], J.M. Le Goff [a], L. Leistam [a], R. Leiste [ak], M. Lenti [b], E. Leonardi [q], J. Lettry [i], P.M. Levchenko [k], X. Leytens [x], C. Li [h,af], H.T. Li [ae], J.F. Li [h], L. Li [ai], P.J. Li [aj], Q. Li [h], X.G. Li [ae], J.Y. Liao [aj], Z.Y. Lin [af], F.L. Linde [x,a], B. Lindemann [w], D. Linnhofer [i], R. Liu [h], Y. Liu [h], W. Lohmann [ak], E. Longo [q], Y.S. Lu [ae], J.M. Lubbers [a], K. Lübelsmeyer [w], C. Luci [a], D. Luckey [j,m], L. Ludovici [q], L. Luminari [q], W.G. Ma [af], M. MacDermott [i], R. Magahiz [ap], P.K. Malhotra [p], R. Malik [h], A. Malinin [u,n], C. Maña [c], D.N. Mao [o], Y.F. Mao [ae], M. Maolinbay [i], P. Marchesini [i], A. Marchionni [b], J.P. Martin [aa], L. Martinez-Laso [a],

F. Marzano[q], G.G.G. Massaro[x], T. Matsuda[j], K. Mazumdar[p], P. McBride[ao], T. McMahon[ab], D. McNally[i], Th. Meinholz[w], M. Merk[ah], L. Merola[e], M. Meschini[b], W.J. Metzger[ah], Y. Mi[h], G.B. Mills[an], Y. Mir[h], G. Mirabelli[q], J. Mnich[w], M. Möller[w], B. Monteleoni[b], G. Morand[t], R. Morand[u], S. Morganti[q], N.E. Moulai[h], R. Mount[am], S. Müller[w], E. Nagy[v], M. Napolitano[e], H. Newman[am], C. Neyer[i], M.A. Niaz[h], L. Niessen[w], H. Nowak[ak], D. Pandoulas[w], M. Pauluzzi[g], F. Pauss[i], F. Plasil[ag], G. Passaleva[b], G. Paternoster[e], S. Patricelli[e], Y.J. Pei[w], D. Perret-Gallix[u], J. Perrier[t], A. Pevsner[d], M. Pieri[b], P.A. Piroué[r], V. Plyaskin[n], M. Pohl[i], V. Pojidaev[n], N. Produit[t], J.M. Qian[o], K.N. Qureshi[h], R. Raghavan[p], G. Rahal-Callot[i], G. Raven[x], P. Razis[s], K. Read[ag], D. Ren[i], Z. Ren[h], S. Reucroft[f], A. Ricker[w], S. Riemann[ak], O. Rind[o], C. Rippich[z], H.A. Rizvi[h], B.P. Roe[o], M. Röhner[w], S. Röhner[w], L. Romero[c], J. Rose[w], S. Rosier-Lees[u], R. Rosmalen[ah], Ph. Rosselet[a,l], A. Rubbia[j], J.A. Rubio[c,a], W. Ruckstuhl[t], H. Rykaczewski[i], M. Sachwitz[a,ak], J. Salicio[c,a], J.M. Salicio[c], G. Sanders[an], A. Santocchia[g], M.S. Sarakinos[j], G. Sartorelli[h,m], G. Sauvage[u], A. Savin[n], V. Schegelsky[k], K. Schmiemann[w], D. Schmitz[w], P. Schmitz[w], M. Schneegans[u], H. Schopper[aq], D.J. Schotanus[ah], S. Shotkin[j], H.J. Schreiber[ak], R. Schulte[w], S. Schulte[w], K. Schultze[w], J. Schütte[ao], J. Schwenke[w], G. Schwering[w], C. Sciacca[e], I. Scott[ao], R. Sehgal[h], P.G. Seiler[ai], J.C. Sens[x], L. Servoli[g], I. Sheer[y], D.Z. Shen[aj], V. Shevchenko[n], S. Shevchenko[n], X.R. Shi[am], K. Shmakov[n], V. Shoutko[n], E. Shumilov[n], N. Smirnov[k], E. Soderstrom[r], A. Sopczak[y], C. Spartiotis[d], T. Spickermann[w], P. Spillantini[b], R. Starosta[w], M. Steuer[j,m], D.P. Stickland[r], F. Sticozzi[j], W. Stoeffl[ac], H. Stone[t], K. Strauch[ao], B.C. Stringfellow[ab], K. Sudhakar[w,p], G. Sultanov[h], R.L. Sumner[r], L.Z. Sun[h,af], H. Suter[i], R.B. Sutton[z], J.D. Swain[h], A.A. Syed[h], X.W. Tang[ae], E. Tarkovsky[n], L. Taylor[f], C. Timmermans[ah], Samuel C.C. Ting[j], S.M. Ting[j], Y.P. Tong[ad], F. Tonisch[ak], M. Tonutti[w], S.C. Tonwar[p], J. Tóth[a,v], G. Trowitzsch[ak], C. Tully[am], K.L. Tung[ae], J. Ulbricht[i], L. Urbán[v], U. Uwer[w], E. Valente[q], R.T. Van de Walle[ah], I. Vetlitsky[n], G. Viertel[i], P. Vikas[h], U. Vikas[h], M. Vivargent[j,u], H. Vogel[z], H. Vogt[ak], G. Von Dardel[a], I. Vorobiev[n], A.A. Vorobyov[k], An.A. Vorobyov[k], L. Vuilleumier[a,l], M. Wadhwa[h], W. Wallraff[w], C.R. Wang[af], G.H. Wang[z], J.H. Wang[ae], Q.F. Wang[ao], X.L. Wang[af], Y.F. Wang[b], Z. Wang[h], Z.M. Wang[af,h], A. Weber[w], J. Weber[i], R. Weill[a,l], T.J. Wenaus[ac], J. Wenninger[t], M. White[j], C. Willmott[c], F. Wittgenstein[a], D. Wright[r], R.J. Wu[ae], S.L. Wu[h], S.X. Wu[h], Y.G. Wu[ae], B. Wysłouch[j], Y.Y. Xie[aj], Y.D. Xu[ae], Z.Z. Xu[af], Z.L. Xue[aj], D.S. Yan[aj], X.J. Yan[j], B.Z. Yang[af], C.G. Yang[ae], G. Yang[h], K.S. Yang[ae], Q.Y. Yang[ae], Z.Q. Yang[aj], C.H. Ye[h], J.B. Ye[af,i], Q. Ye[h], S.C. Yeh[ad], Z.W. Yin[aj], J.M. You[h], M. Yzerman[x], C. Zaccardelli[am], P. Zemp[i], M. Zeng[h], Y. Zeng[w], D.H. Zhang[x], Z.P. Zhang[h,af], J.F. Zhou[w], R.Y. Zhu[am], H.L. Zhuang[ae] and A. Zichichi[h,a,m]

[a] *European Laboratory for Particle Physics, CERN, CH-1211 Geneva 23, Switzerland*
[b] *INFN – Sezione di Firenze and University of Firenze, I-50125 Florence, Italy*
[c] *Centro de Investigaciones Energeticas, Medioambientales y Tecnologicas, CIEMAT, E-28040 Madrid, Spain*
[d] *Johns Hopkins University, Baltimore, MD 21218, USA*
[e] *INFN – Sezione di Napoli and University of Naples, I-80125 Naples, Italy*
[f] *Northeastern University, Boston, MA 02115, USA*
[g] *INFN – Sezione di Perugia and Universitá Degli Studi di Perugia, I-06100 Perugia, Italy*
[h] *World Laboratory, FBLJA Project, CH-1211 Geneva, Switzerland*
[i] *Eidgenössische Technische Hochschule, ETH Zürich, CH-8093 Zurich, Switzerland*
[j] *Massachusetts Institute of Technology, Cambridge, MA 02139, USA*
[k] *Leningrad Nuclear Physics Institute, SU-188 350 Gatchina, USSR*
[l] *Central Laboratory of Automation and Instrumentation, CLANP, Sofia, Bulgaria*
[m] *INFN – Sezione di Bologna, I-40126 Bologna, Italy*
[n] *Institute of Theoretical and Experimental Physics, ITEP, SU-117 259 Moscow, USSR*
[o] *University of Michigan, Ann Arbor, MI 48109, USA*

[p] *Tata Institute of Fundamental Research, Bombay 400 005, India*
[q] *INFN – Sezione di Roma and University of Rome "La Sapienza", I-00185 Rome, Italy*
[r] *Princeton University, Princeton, NJ 08544, USA*
[s] *University of Alabama, Tuscaloosa, AL 35486, USA*
[t] *University of Geneva, CH-1211 Geneva 4, Switzerland*
[u] *Laboratoire de Physique des Particules, LAPP, F-74519 Annecy-le-Vieux, France*
[v] *Central Research Institute for Physics of the Hungarian Academy of Sciences, H-1525 Budapest 114, Hungary*
[w] *I. Physikalisches Institut, RWTH, W-5100 Aachen, FRG*[1]
and III. Physikalisches Institut, RWTH, W-5100 Aachen, FRG[1]
[x] *National Institute for High Energy Physics, NIKHEF, NL-1009 DB Amsterdam, The Netherlands*
[y] *University of California, San Diego, CA 92182, USA*
[z] *Carnegie Mellon University, Pittsburgh, PA 15213, USA*
[aa] *Institut de Physique Nucléaire de Lyon, IN2P3-CNRS/Université Claude Bernard, F-69622 Villeurbanne Cedex, France*
[ab] *Purdue University, West Lafayette, IN 47907, USA*
[ac] *Lawrence Livermore National Laboratory, Livermore, CA 94550, USA*
[ad] *High Energy Physics Group, Taiwan, ROC*
[ae] *Institute of High Energy Physics, IHEP, Beijing, China*
[af] *University of Science and Technology of China, Hefei, Anhui 230 029, China*
[ag] *Oak Ridge National Laboratory, Oak Ridge, TN 37830, USA*
[ah] *University of Nijmegen and NIKHEF, NL-6525 ED Nijmegen, The Netherlands*
[ai] *Paul Scherrer Institut (PSI), Würenlingen, Switzerland*
[aj] *Shanghai Institute of Ceramics, SIC, Shanghai, China*
[ak] *Institut für Hochenergiephysik, O-1615 Zeuthen-Berlin, FRG*[1]
[al] *University of Lausanne, CH-1015 Lausanne, Switzerland*
[am] *California Institute of Technology, Pasadena, CA 91125, USA*
[an] *Los Alamos National Laboratory, Los Alamos, NM 87544, USA*
[ao] *Harvard University, Cambridge, MA 02139, USA*
[ap] *Union College, Schenectady, NY 12308, USA*
[aq] *University of Hamburg, W-2000 Hamburg, FRG*

Received 18 June 1991

From 2540 $Z^0 \to \tau^+\tau^-$ events, we determine the inclusive decay branching fractions of the τ-lepton into one and three charged particles to be 0.856 ± 0.006 (stat.) ± 0.003 (syst.) and 0.144 ± 0.006 (stat.) ± 0.003 (syst.), respectively. The leptonic branching fractions are measured to be 0.175 ± 0.008 (stat.) ± 0.005 (syst.) for $\tau \to \mu\nu_\mu\nu_\tau$ and 0.177 ± 0.007 (stat.) ± 0.006 (syst.) for $\tau \to e\nu_e\nu_\tau$. We determine the τ lifetime both from three-prong decays using the decay length and from one-prong decays using the impact parameter. The results from the two independent methods agree and yield a combined value of $[0.309 \pm 0.023$ (stat.) ± 0.030 (syst.)$] \times 10^{-12}$s.

Introduction

The decays of heavy leptons are well suited to study the strength and structure of the weak charged current. Since the pioneering search for sequential heavy leptons by measurement of e–μ final states [1], and the subsequent discovery of the τ-lepton in e^+e^- reactions [2], much information about its properties has been accumulated [3].

The L3 collaboration has previously presented the measurements of the cross sections for $e^+e^- \to Z^0 \to \tau^+\tau^-$ [4] at energies around the Z^0 resonance. Here we analyze the same event sample to measure the topological and leptonic branching fractions of the τ decay and the τ lifetime. Since our selection of τ candidates used for the cross section measurement is largely based on calorimetric information rather than charged multiplicity, the topological branching fractions can be extracted with small systematic biases. Because of the high center-of-mass energy of LEP, the background contribution from low multiplicity hadronic events is small. The good resolution

[1] Supported by the German Bundesministerium für Forschung und Technologie.

of the central detector yields a measurement of the τ lifetime competitive with previous high statistics determinations at lower energies [5].

The L3 detector

The L3 detector consists of a central tracking chamber, a high-resolution electromagnetic calorimeter composed of BGO crystals, a ring of scintillation counters, a uranium and brass hadron calorimeter with proportional wire chamber readout, and an accurate muon chamber system. These detectors are installed in a 12 m diameter magnet which provides a uniform field of 0.5 T along the beam direction.

The central tracking chamber is a time expansion chamber (TEC) which consists of two cylindrical layers of 12 and 24 sectors, with 62 wires measuring the R/ϕ coordinate. The chamber is separated from the beam line by two concentric beryllium tubes of 1.5 mm thickness. The first coordinate is measured at a distance of 109.8 mm from the beam line, the last one at a distance of 427.2 mm. The single-wire resolution is 58 μm averaged over the entire cell. The double-track resolution is 640 μm. The fine segmentation of the BGO detector and the hadron calorimeter allow us to measure the direction of taus from the thrust axis of tau decay products with an angular resolution of 1.8°. The muon detector consists of 3 layers of precise drift chambers.

For the present analysis, we use the data collected in a fiducial region covered by the electromagnetic barrel calorimeter, i.e. $-0.7 < \cos\theta_T < 0.7$, where θ_T is the polar angle of the event's thrust axis.

A detailed description of each detector subsystem, and its performance, is given in ref. [6].

Determination of the topological branching fractions

The event selection [4] of $Z^0 \rightarrow \tau^+\tau^-$ is mainly based on calorimetric quantities. The selection criteria are:

(1) The total energy deposited in the electromagnetic calorimeter is required to be greater than 2 GeV and less than 60 GeV.

(2) The number of clusters reconstructed in the electromagnetic calorimeter must be less than 13 and the number of charged tracks in the TEC must be less than 9.

(3) The event is required to have at least one scintillation counter hit within 6 ns of the beam gate.

(4) The event must contain at least two and at most three jets, each with an energy greater than 3 GeV.

(5) The acollinearity angle between the two most energetic jets must be less than 14°.

(6) The event is required to have no more than one isolated muon and, in addition, the muon must have a momentum of less than $0.88E_{beam}$.

(7) If the shower profile of a jet is consistent with an electron or a photon, the energy deposited in the BGO associated with that jet must be less than $0.88E_{beam}$.

There are 2540 events passing these cuts, which correspond to an efficiency of 75.4% within the fiducial region [4]. Fig. 1 shows an example of a $Z^0 \rightarrow \tau^+\tau^-$ event as observed in the L3 central tracking chamber and electromagnetic calorimeter, where one τ decays into an electron and the other into three charged hadrons. The three tracks from this decay are clearly

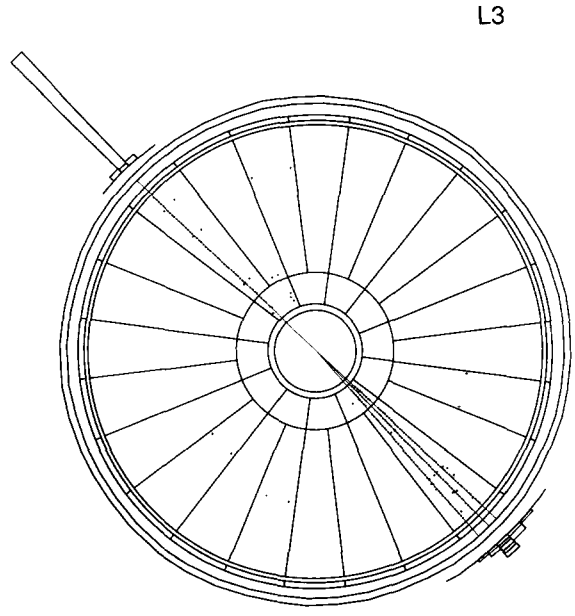

Fig. 1. Display of a $Z^0 \rightarrow \tau^+\tau^-$ event in the central tracking chamber of L3. Hits and reconstructed tracks in the TEC are shown. Used hits are shown as dots, and unused hits as crosses. The polar histogram represents the energy depositions in the BGO calorimeter. One τ decays into an electron, while the other τ decays into three charged hadrons.

separated.

For the multiplicity measurement we require that there be at least one well measured track present in the event. A well measured track for this analysis fulfills the following criteria: (a) a good circle fit in the R/ϕ projection with a length of at least 216 mm; (b) at least 30 out of a maximum of 62 hits used in the track fit; (c) distance of closest approach (DCA) to average beam position less than 10 mm. The event is then divided into two hemispheres, separated by the plane normal to the thrust axis. The multiplicity is counted in each hemisphere.

The efficiencies to detect the one-prong, three-prong or five-prong decays of the tau are calculated with Monte Carlo simulations [7]. The detector simulation includes the effects of the chamber's resolution, double-track resolution and efficiency as observed during the 1990 running period. Applying the selection described above, the probabilities e_i to accept a decay from each of the three topological channels $i = 1, 3, 5$ are determined to be $(74.5 \pm 0.3)\%$, $(80.7 \pm 0.6)\%$ and $(76.5 \pm 1.6)\%$, respectively, inside the fiducial region. The error bars are statistical errors only. The simulation also allows a determination of the probabilities ϵ_{ij} to observe j tracks, when i charged particles were produced in the decay. For background estimation, also Z^0 decays into e^+e^-, $\mu^+\mu^-$ and hadrons are simulated and submitted to the same selection criteria as $\tau^+\tau^-$ candidates. This simulation determines the small fractions c_k accepted from the three background channels k as well as the probabilities δ_{kj} to observe j tracks from these sources. All other background sources are negligible. The prediction of the observed multiplicity distribution

$$n_{expected}(j) = \frac{(1-\sum_k c_k)\sum_i \mathrm{BR}_i e_i \epsilon_{ij} + \sum_k c_k \delta_{kj}}{(1-\sum_k c_k)\sum_i \mathrm{BR}_i e_i + \sum_k c_k} n_\tau, \qquad (1)$$

where n_τ is the total number of τ decays included in the sample, is then fitted to the observed multiplicity distribution. The free parameters of the fit are the branching fractions BR_1 and BR_3 for τ decays into one and three charged particles respectively. The branching fraction into five charged particles is then given as $\mathrm{BR}_5 = 1 - \mathrm{BR}_1 - \mathrm{BR}_3$. Fig. 2a shows the measured charge multiplicity distribution. Note the large peaks at one and three prongs as expected. However, because of the difficulty simulating the double-track resolution in the regions on borders of TEC sectors, the Monte Carlo is in only fair agreement with our observations. We therefore choose to eliminate the border regions which are within 15 mrad of the anode and cathode plane of TEC sectors from our fiducial region. After the cut, the Monte Carlo reproduces the measured double-track resolution well. Our track efficiency then drops, as seen in fig. 2b, but we are able to simulate the charge multiplicity distribution well as seen from the better agreement between data and Monte Carlo in the figure. The χ^2 of the fit is 2.0 for 4 degrees of freedom. The cut changes the fitted branching fractions by less than their statistical errors.

A contribution to the systematic error on the measured branching fractions comes from the uncertainty in the Monte Carlo determination of the parameters e_i, ϵ_{ij} and δ_{kj} of the fitting function. Their errors produce uncertainties in the three branching fractions of ± 0.0015, ± 0.0006 and ± 0.0005. Varying the background fractions c_k within one standard deviation changes the results by ± 0.002, ± 0.002 and ± 0.001. The influence of the exclusion of regions around the anode and cathode planes has been studied by varying the cut between 10 mrad and 20 mrad. The resulting variations of the branching fractions are ± 0.002, ± 0.002 and ± 0.001. The effect of the excluded regions depends slightly on the kinematics of the decays into three or more charged particles. To estimate the magnitude of this dependence, the dominant decays of $\tau^\pm \to a_1\, \nu_\tau \to 3$ charged particles + neutrals and $\tau^\pm \to n\pi\nu_\tau \to 3$ charged particles + neutrals were simulated separately. Varying the ratio of the two decay modes by its uncertainty produced negligible systematic changes in BR_3 (± 0.0002). The resulting topological branching fractions are then

$$\mathrm{BR}(\tau^\pm \to 1 \text{ charged particle} + \text{neutrals}) = 0.856 \pm 0.006 \pm 0.003,$$

$$\mathrm{BR}(\tau^\pm \to 3 \text{ charged particles} + \text{neutrals}) = 0.144 \pm 0.006 \pm 0.003.$$

The first error is statistical, the second is systematic.

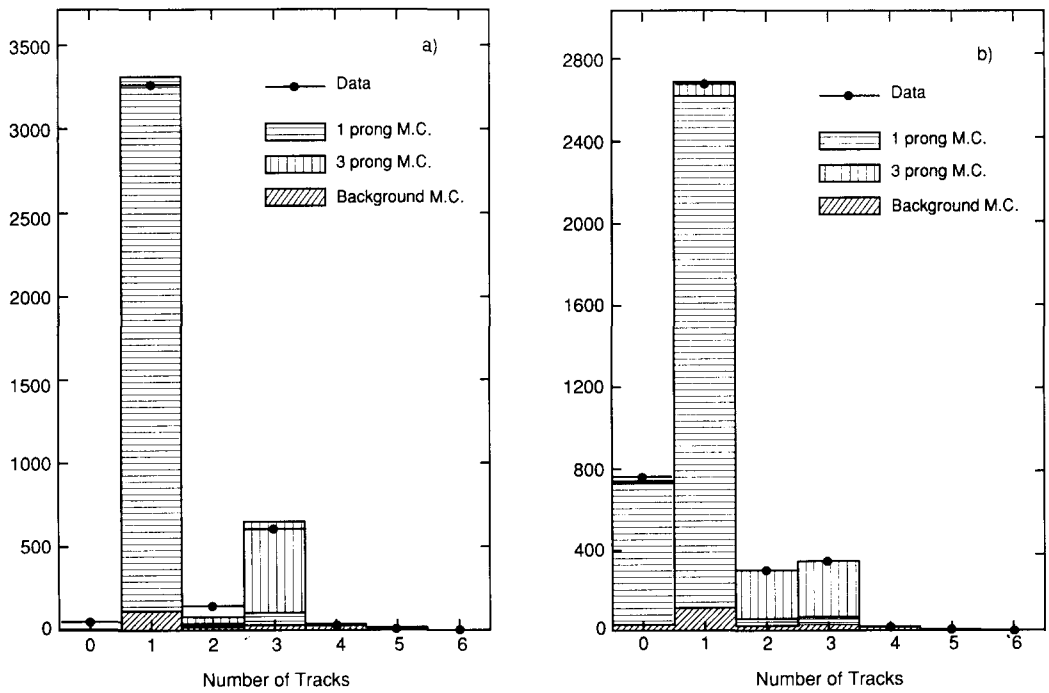

Fig. 2. The charged multiplicity distribution for observed τ decay candidates (points) compared to the best fit of the expected distribution (histogram), where the different hatchings show the contributions from one-prong and three-prong τ decays as well as backgrounds from $Z^0 \to e^+e^-$, $\mu^+\mu^-$ and hadrons: (a) before exclusion of the boundary regions; (b) after exclusion of the boundary regions as described in the text.

Thus

$$BR(\tau^{\pm} \to 5 \text{ charged particles} + \text{neutrals}) < 0.0034 \ (95\% \text{ CL}).$$

These results are in agreement with the current world averages [3].

Determination of the leptonic branching fractions

To identify electrons and muons from τ decay additional selection criteria are applied to our τ sample. The criteria are applied independently in each hemisphere of the event.

To identify muons, we require a reconstructed track in the muon chambers with a momentum greater than 2 GeV which extrapolates back to the interaction point within 10 cm along and transverse to the beam direction. A candidate is then accepted as a muon if the energy deposited in the hadron calorimeter is less than 6 GeV.

To identify electrons we require that the shower profile of a candidate in the electromagnetic calorimeter be consistent with that expected from a purely electromagnetic shower. The energy deposited in the hadron calorimeter is required to be less than 5 GeV. And there must be at most one good track which matches the center-of-gravity of the cluster within 8 mrad in the transverse plane.

After applying the above criteria, 624 events with at least one muon and 686 events with at least one electron have been found and used for the calculation of the branching fractions. The selection efficiencies and background fractions from other channels as estimated from Monte Carlo simulation are shown in table 1. The numbers are given as fractions of the total number of τ events produced inside the fiducial region, where exactly one τ decays leptonically.

Figs. 3 and 4 show the spectra of electrons and

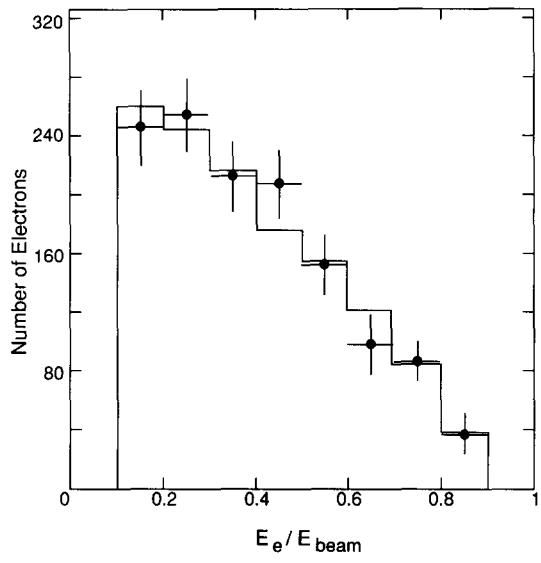

Fig. 3. The energy distribution for electrons from selected τ decays (points) compared to the distribution expected from Monte Carlo (histogram). The distribution has been acceptance corrected and background events are subtracted.

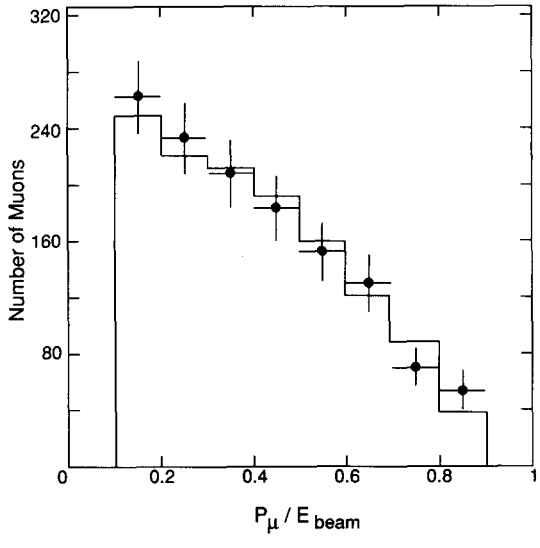

Fig. 4. The momentum distribution for muons from selected τ decays (points) compared to the distribution expected by Monte Carlo (histogram). The distribution has been acceptance corrected and background events are subtracted.

Table 1
Selection efficiencies from Monte Carlo for leptonic τ decays, hadronic τ decays and dilepton background processes.

ℓ	$\tau \to \ell$	$\tau \to$ hadrons	$Z^0 \to \ell^+\ell^-$
μ	63.0%	2.0%	0.4%
e	60.6%	3.9%	1.0%

muons from τ decay compared with the expectations determined by Monte Carlo. The distributions have been corrected for acceptance and the backgrounds have been subtracted.

The final branching fractions after taking into account the efficiency corrections and background subtractions are determined to be

$$\mathrm{BR}(\tau \to \mu\nu_\mu\nu_\tau) = 0.175 \pm 0.008 \pm 0.005,$$

$$\mathrm{BR}(\tau \to e\nu_e\nu_\tau), = 0.177 \pm 0.007 \pm 0.006,$$

where the first error is statistical, the second systematic. This systematic error was estimated by varying the cuts and the background fractions by their estimated uncertainties to account for any imperfections in the Monte Carlo simulation. The results are in excellent agreement with the current world average values of 0.178 ± 0.004 and 0.177 ± 0.004, respectively [3].

The measured ratio, $\Gamma(\tau \to \mu\nu_\mu\nu_\tau)/\Gamma(\tau \to e\nu_e\nu_\tau) = 0.986 \pm 0.063$, is in agreement with the expectation of 0.973 from e–μ–τ universality in the weak charged current [8].

These measurements can be used to estimate the value of the strong coupling constant, $\alpha_s(Q^2)$ at $Q^2 = m_\tau^2$. The quantity R^τ_{had} is defined as the ratio

$$R^\tau_{\mathrm{had}} = \frac{\Gamma(\tau \to \text{hadrons}\ \nu_\tau)}{\Gamma(\tau \to e\nu_e\nu_\tau)} = \frac{1 - B^\tau_e - B^\tau_\mu}{B^\tau_e}.$$

Using the leptonic branching fractions, we obtain $R^\tau_{\mathrm{had}} = 3.64^{+0.25}_{-0.23}$. R^τ_{had} has been computed in perturbative QCD to third order in α_s [9]. Both non-perturbative effects, which have been found to be small, and weak corrections have been calcu-

lated [10,11]. Using the theoretical expression for R^{τ}_{had} [11], we derive

$$\alpha_s(Q^2 = m_\tau^2) = 0.34^{+0.07}_{-0.09}.$$

A comparison with the number $\alpha_s(Q^2 = m_Z^2) = 0.125 \pm 0.041$ [4], obtained from a measurement of the ratio R^{Z}_{had} defined in analogy to R^{τ}_{had}, confirms the running of α_s as predicted by QCD. Extrapolating the α_s values from $Q^2 = m_\tau^2$ to m_Z^2 yields [12,3]

$$\alpha_s(m_Z^2) = 0.118^{+0.007}_{-0.012}.$$

This number is in agreement with our determination of the strong coupling constant from an analysis of the topology of hadronic Z^0 decays, $\alpha_s = 0.115 \pm 0.009$ [13].

Lifetime measurement from three-prong decays

To determine the lifetime of the τ-lepton, we first use its decays into three charged particles. In this determination, we measure the decay distance of the τ using the average position of the beam spot as its origin and the vertex determined from the decay products as its decay point. All these measurements are made in the plane transverse to the beam direction.

The average position of the beam spot in the L3 intersection point is measured for each LEP fill using good quality tracks in hadronic events. Its position is determined by minimizing the sum of the squared distances of well measured high transverse momentum tracks to a common origin. This method yields the average beam position within each fill with a mean uncertainty of less than 46 μm, as estimated from the variations in the vertical beam position between consecutive LEP fills.

The size of the beam spot is determined from high transverse momentum tracks from the reactions $e^+e^- \to e^+e^-$ and $e^+e^- \to \mu^+\mu^-$. The distribution of their DCA to the average beam position measures the size of the beam spot folded with the experimental resolution on track parameters as well as average beam position. The distance between the two tracks at the average beam position measures the experimental resolution on the DCA alone. By unfolding the contributions from the size of the beam spot and the experimental resolution we obtain an effective RMS beam spot size of $\sigma_x = (196 \pm 5)$ μm in the horizontal direction and $\sigma_y = (24 \pm 25)$ μm in the vertical direction. These numbers contain the uncertainty in the determination of the mean beam position.

The average RMS error on the distance of closest approach is $\bar{\sigma}_{DCA} = (144 \pm 1)$ μm for particle momenta of 45 GeV. For lower momenta, a small additional contribution from multiple scattering inside the beryllium beam pipe is taken into account.

In selecting three-prong decays of the τ for the lifetime measurement, we make the following additional requirements to the sample of 2540 events:

- There must be three well measured tracks in one hemisphere, as determined by the event's thrust axis, with a maximum opening angle between any two of 15°.
- There must be one or three tracks in the opposite hemisphere.
- All tracks must have at least two hits in the inner layers of the chamber.
- The vertex from the three charged tracks must be determined with a χ^2 probability larger than 5% and with an error along the direction of flight of less than 10 mm.

After these additional criteria, a total of 251 candidates for three-prong decays remain. The background from other reactions in this sample is determined by Monte Carlo to be less than one event.

Fig. 5 shows the distribution of the distance between the average position of the beam spot and the τ decay vertex – the decay distance distribution – for these candidates. The sign of the decay distance is defined such that decay vertices in the τ-production hemisphere acquire a positive sign and those in the opposite hemisphere a negative sign. The measured projection of the decay distance onto the transverse plane is then divided by $\sin\theta_T$, where θ_T is the production angle approximated by the polar angle of the event's thrust axis. Also shown in fig. 5 is the result of an unbinned maximum likelihood fit, which uses an event probability density p proportional to the theoretical decay distance distribution folded with a gaussian resolution

$$p(d_i) = \frac{1}{\sqrt{2\pi}\sigma_i\lambda} \int_0^\infty e^{-x/\lambda} e^{-(x-\lambda_i)^2/2\sigma_i^2} dx, \qquad (2)$$

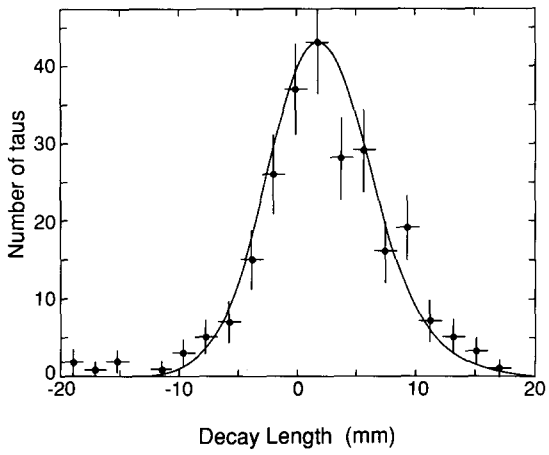

Fig. 5. The decay length distribution for τ decays into three charged particles (points) compared to the expected distribution (line) determined by an unbinned maximum likelihood fit.

where λ is the τ decay length and λ_i is the decay distance measured in event i. The error on this distance, σ_i, takes into account the contributions from both the size of the beam spot and the error on the decay vertex as determined from the covariance matrices of the track parameters.

The likelihood function is then the product of these probability densities for all events and is maximized with respect to the decay length λ. Using the average momentum of τ-leptons in our sample of $(98.8 \pm 0.1)\%$ of the beam energy, as determined from Monte Carlo including radiative corrections, we thus obtain a first result for the τ lifetime

$$\tau_\tau = (0.302 \pm 0.036) \times 10^{-12}\text{s},$$

where the error is statistical only.

Systematic errors in this measurement occur mainly by miscalibration of the central tracking chamber and by systematic under or overestimation of the decay distance error σ_i. Varying the two main parameters of the chamber's time-distance relation, i.e. the drift velocity and the zero point of the drift time measurement, by the estimated systematic uncertainties (0.2% and 5 ns, respectively) around their calibrated values, we obtain a relative variation of the determined decay length of 2% and 2.5%, respectively. Systematically scaling the error σ_i of the decay length in each event by a factor deviating from one by $\pm 20\%$, we observe a relative variation of the decay length of $\pm 5\%$. This factor is estimated to cover uncertainties in the determination of the track parameter errors as well as systematic deviations of the single-hit position error from its estimated behavior. We thus conclude that this method determines the τ lifetime with a systematic uncertainty of $\pm 0.021 \times 10^{-12}$s.

Lifetime measurement from one-prong decays

As a second, independent method we determine the τ lifetime from a measurement of the impact parameter in one-prong decays. The impact parameter δ of a track is given by the DCA to the average beam position in a fill, signed positive if the track intersects with the event's thrust axis in the direction of flight of the τ and signed negative if it intersects opposite to this direction. It is divided by $\sin\theta_T$, θ_T being the τ's production angle, since the DCA is measured in the projection onto the transverse plane.

The candidates for this measurement are selected in the same way as those for three-prong decays, except that exactly one track is required in each hemisphere of the event and that each track must have a DCA to the average beam position of less than 1.5 mm. The sample then consists of 2566 candidates for τ decay into one charged particle with an estimated background of $(1.35 \pm 0.70)\%$.

Fig. 6 shows the distribution of the impact parameter δ_i for these events. The sample is subjected to an unbinned maximum likelihood fit with an event probability density analogous to eq. (2) to determine the average impact parameter δ:

$$p(\delta_i) = \frac{1}{\sqrt{2\pi}\sigma_i\delta} \int_0^\infty e^{-x/\delta} e^{-(x-\delta_i)^2/2\sigma_i^2} dx. \qquad (3)$$

Here, σ_i is the error of the impact parameter measurement, folded with the RMS size of the beam spot in the flight direction of the τ. The resulting average impact parameter value for the data is $\delta = (64 \pm 6)\ \mu$m.

The conversion of the quantity δ into a τ lifetime is less direct than in the case of the decay distance measurement and proceeds via Monte Carlo. For this purpose, high-statistics samples of $e^+e^- \to Z^0 \to$

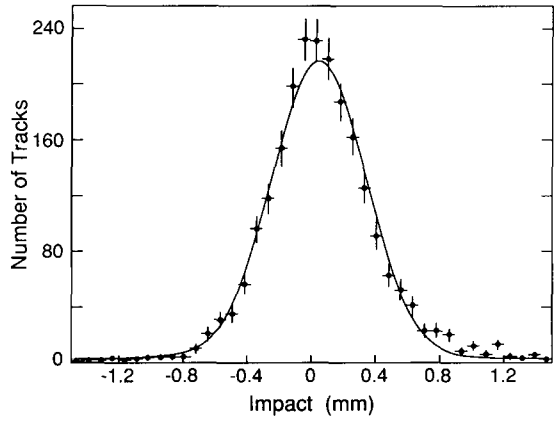

Fig. 6. The impact parameter distribution for τ decays into one charged particle (points) compared to the expected distribution (line) determined by an unbinned maximum likelihood fit.

$\tau^+\tau^-$ with τ lifetimes between 0.004×10^{-12}s and 0.604×10^{-12}s have been generated, the detector response simulated [7] and the simulated events run through the same analysis as the data. The relation between the average impact parameter δ and the lifetime τ_τ is thus determined to be

$$\delta = [(-1.4 \pm 1.9) + (207 \pm 6)\tau_\tau(10^{-12}\text{s})]\ \mu\text{m}. \quad (4)$$

The bias for a lifetime of zero can be cross-checked using the distribution of a sample of tracks from hadronic Z^0 decays fulfilling cuts analogous to those for τ decays, which yields $\delta^0 = (7 \pm 4)\ \mu$m.

This method thus yields a τ lifetime

$$\tau_\tau = (0.318 \pm 0.028) \times 10^{-12}\text{s},$$

where the error is statistical only. The expected δ-distribution corresponding to the best fit is overlayed on fig. 6. A systematic error is again estimated by varying the parameters of the time-distance relation as above to cover the influence of the chamber calibration. An error of $\pm 0.018 \times 10^{-12}$s from the uncertainty of the drift velocity and of $\pm 0.010 \times 10^{-12}$s from the time-zero results. In addition, a systematic error of $\pm 0.014 \times 10^{-12}$s from the uncertainty in the parameters of eq. (4) has to be taken into account. The uncertainty of the beam position per fill is included in the impact errors σ_i entering into the likelihood calculation. If the track parameter errors are varied by the estimated systematic uncertainties of $\pm 7\%$ around their values determined from ee and $\mu\mu$ events, the resulting lifetime changes by $\pm 0.026 \times 10^{-12}$s. We thus estimate a total systematic error for the impact parameter method of $\pm 0.037 \times 10^{-12}$s.

Since the samples for both methods are exclusive, the two results can be combined. The systematic errors from calibration and error determination are correlated, while the others are not. Taking into account this correlation, we obtain a combined result for the τ lifetime

$$\tau_\tau = (0.309 \pm 0.023 \pm 0.030) \times 10^{-12}\text{s},$$

where the first error is statistical, and the second systematic. This result agrees with the current world average of $(0.303 \pm 0.008) \times 10^{-12}$s [3]. The measurement also agrees with the theoretical expectation from the standard model

$$\tau_\tau = \tau_\mu \left(\frac{G_F^\mu}{G_F^\tau}\right)^2 \left(\frac{m_\mu}{m_\tau}\right)^5 \text{BR}(\tau \to \text{e}\nu_\text{e}\nu_\tau), \quad (5)$$

where τ_μ is the measured muon lifetime and G_F^μ and G_F^τ are the Fermi coupling constants of μ and τ. This relation is affected by standard model radiative corrections only at the percent level [14]. Using our own result on the τ branching fraction into electrons, the relation predicts a τ lifetime of $(0.283 \pm 0.016) \times 10^{-12}$s for equal coupling constants to the weak charged current. Converting relation (5) into a measurement of the coupling constant ratio, we obtain

$$\frac{G_F^\mu}{G_F^\tau} = 1.04 \pm 0.07.$$

Conclusions

We have analyzed $Z^0 \to \tau^+\tau^-$ decays and determined the topological and leptonic branching fractions as well as the τ lifetime. The results are in good agreement with previous measurements at lower energies. They are also compatible with expectations from the standard model based on the assumption of e–μ–τ universality of the weak charged current couplings.

Acknowledgment

Those of us who are not from member states wish to thank CERN for its hospitality and help. We want to express our gratitude to the CERN LEP division: it is their excellent achievements which made this experiment possible. We acknowledge the effort of all engineers and technicians who have participated in the construction and maintenance of this experiment.

References

[1] A. Zichichi et al., INFN/AE-67/3 (March 1967); Nuovo Cimento A 17(1973) 383.
[2] M. L. Perl et al., Phys. Rev. Lett. 35 (1975) 1489.
[3] See M. Aguilar-Benitez et al., Phys. Lett. B 239 (1990) 1, and references therein.
[4] L3 Collab., B. Adeva et al., L3 preprint # 28 (February 1991), to be published in Z. Phys.
[5] H. Albrecht et al., Phys. Lett. B 232 (1989) 554;
C. Kleinwort et al., Z. Phys. C 42 (1989) 7;
W. Braunschweig et al., Z. Phys. C 39 (1988) 331;
D. Amidei et al., Phys. Rev. D 37 (1988) 1750;
H. Albrecht et al., Phys. Lett. B 199 (1987) 580;
C. Bebek et al., Phys. Rev. D 36 (1987) 690;
S. Abachi et al., Phys. Rev. Lett. 59 (1987) 2519;
H. R. Band et al., Phys. Rev. Lett. 59 (1987) 415;
E. Fernandez et al., Phys. Rev. Lett. 54 (1985) 1624.
[6] L3 Collab., B. Adeva et al., Nucl. Instrum. Methods A 289 (1990) 35.
[7] The event generation is based on Koralz Version 3.7, see S. Jadach et al., Z Physics at LEP 1, CERN Report CERN-89-08, Vol. 3 (1989) 69.
The L3 detector simulation is based on GEANT Version 3.13 (September 1989), see R. Brun et al., GEANT 3, CERN DD/EE/84-1 (revised) (September 1987).
Hadronic interactions are simulated based on the GHEISHA program, see H. Fesefeldt, RWTH Aachen PITHA 85/02 (1985).
[8] H.B. Thacker and J.J. Sakurai, Phys. Lett. B 36 (1971) 103.
[9] L.R. Surguladze and M.A. Samuel, Phys. Rev. Lett. 66 (1991) 56;
S.G. Gorishny, A.L. Kataev and S.A. Larin, Phys. Lett. B 259 (1991) 144.
[10] E. Braaten and C.S. Li, Phys. Rev. D 42 (1990) 3888;
S. Narison and A. Pich, Phys. Lett. B 211 (1988) 183.
[11] A. Pich, CERN-TH 5940/90.
[12] W. J. Marciano Phys. Rev. D 29 (1984) 580.
[13] L3 Collab., B. Adeva et al. Phys. Lett. B 248 (1990) 464; B 257 (1991) 469.
[14] T.W. Appelquist, J.D. Bjorken and M. Chanowitz Phys. Rev. D 7 (1973) 2225.